Technical University of Denmark

DTU

Rad52 and Rad59 exhibit both overlapping and distinct functions

Feng, Qi; Düring, Louis; Antúnez de Mayolo, Adriana; Lettier, Gaëlle; Lisby, Michael; Erdeniz, Naz; Mortensen, Uffe Hasbro; Rothstein, Rodney

DTU Library
Technical Information Center of Denmark

Rad52 and Rad59 exhibit both overlapping and distinct functions

Qi Feng[a], Louis Düring[b], Adriana Antúnez de Mayolo[a,1], Gaëlle Lettier[c],
Michael Lisby[b], Naz Erdeniz[d], Uffe H. Mortensen[c], Rodney Rothstein[a,*]

[a] Department of Genetics & Development, Columbia University Medical Center, 701 West 168th Street,
New York, NY 10032-2704, USA
[b] Institute of Molecular Biology and Physiology, University of Copenhagen, Øster Farimagsgade 2A,
DK-1353 Copenhagen K, Denmark
[c] Center for Microbial Biotechnology, BioCentrum-DTU, Technical University of Denmark, Building 223,
DK-2800 Lyngby, Denmark
[d] Department of Molecular and Medical Genetics, Oregon Health Sciences University,
3181 SW Sam Jackson Park Road, Mail Code L103, Portland, OR 97201, USA

ARTICLE INFO

ABSTRACT

Homologous recombination is an important pathway for the repair of DNA double-strand breaks (DSBs). In the yeast Saccharomyces cerevisiae, Rad52 is a central recombination protein, whereas its paralogue, Rad59, plays a more subtle role in homologous recombination. Both proteins can mediate annealing of complementary single-stranded DNA in vitro, but only Rad52 interacts with replication protein A and the Rad51 recombinase. We have studied the functional overlap between Rad52 and Rad59 in living cells using chimeras of the two proteins and site-directed mutagenesis. We find that Rad52 and Rad59 have both overlapping as well as separate functions in DSB repair. Importantly, the N-terminus of Rad52 possesses functions not supplied by Rad59, which may account for its central role in homologous recombination.

* Corresponding author. Tel.: +1 212 305 1733; fax: +1 212 923 2090.
  E-mail address: rothstein@cancercenter.columbia.edu (R. Rothstein).
1 Present address: Sylvester Comprehensive Cancer Center, University of Miami Medical Center, 1550 NW 10th Avenue, Miami, FL 33136, USA.

1. Introduction

DNA double-strand break (DSB) repair is essential for protecting genomic integrity in all organisms. In the yeast *Saccharomyces cerevisiae*, the major pathway for DSB repair is homologous recombination (HR). HR is catalyzed by proteins encoded by the *RAD52* epistasis group including *RFA1-3*, *RAD50*, *MRE11*, *XRS2*, *SAE2*, *RAD51*, *RAD52*, *RAD54*, *RAD55*, *RAD57* and *RAD59*. Recombinational repair of DSBs can be explained by two different repair models, the canonical DNA double-strand repair model for homologous recombination that includes a double Holliday junction (dHJ) as a repair intermediate and the synthesis-dependent strand-annealing model that does not involve the formation of a dHJ (reviewed in [1]). A key step in the repair of most DNA DSBs by HR is the strand invasion reaction. *In vitro*, strand invasion can be efficiently performed by the collaborative effort of RPA, Rad51 and Rad52 according to the following scheme: the invasive single-stranded DNA (ssDNA) is bound by RPA to eliminate formation of inhibitory secondary DNA structures. However, RPA binding renders ssDNA inaccessible to Rad51, the recombinase that catalyzes the subsequent strand invasion reaction. Hence, RPA needs to be removed from the ssDNA prior to Rad51 binding. This step is mediated by Rad52, a protein that interacts with both RPA and Rad51 [2–7]. However, strand invasion in living cells is likely to be more complicated because of the participation of other protein factors of the *RAD52* epistasis group. For example, yeast contains a Rad52 paralogue, Rad59, which appears to be a truncated version of Rad52 with homology only to the N-terminal region of Rad52. At present, the functions of Rad59 in DNA DSB repair and HR are poorly understood at the molecular level.

RAD59 was originally discovered on the basis of its role in *RAD51*-independent spontaneous mitotic recombination between inverted repeats [8]. Subsequently, two distinct pathways depending on either Rad59 or Rad51, but both requiring Rad52, have been defined for inverted repeat recombination, recombinational rescue of short telomeres and break-induced replication [8–10]. Homologues of Rad59 have been identified in a number of other organisms including lower eukaryotes, e.g. *Kluyveromyces lactis* and *Eremothecium gossypii* [11,12] and higher eukaryotes, e.g. mouse and human (Rad52B) [13], although it remains unclear whether these homologues are functional equivalents of the yeast protein.

The crystal structure of the N-terminal domain of the *Hs*Rad52 protein has been determined and reveals an undecameric ring [14,15]. The overall structure resembles a mushroom, consisting of a stem that contains highly conserved hydrophobic amino acid residues and a domed cap. By electron microscopy, it has been shown that full-length Rad52 forms heptameric ring structures [16]. Rad52 multimers likely exist *in vivo* since genetic studies have shown that N- and C-terminal *rad52* mutations display intragenic complementation [17,18]. Rad59 has been suggested to form multimers similar to those formed by Rad52 or to form heteromeric rings with Rad52. This view is supported by the findings that Rad59 interacts with Rad52 as well as with itself [19]. Moreover, a sequence comparison of Rad52 and Rad59 reveals that the amino acid residues involved in Rad52 monomer–monomer interaction are the most highly conserved between the two proteins.

The largest difference between Rad52 and Rad59 is the C-terminal extension of Rad52 (amino acids 232–504), which is not conserved in Rad59. This region of Rad52 contains important functions including the Rad51 binding domain [20,21], which is required for Rad52 to efficiently mediate Rad51 catalyzed strand exchange [3]. In agreement with this domain organization, it was found that overexpression of Rad51 suppresses the sensitivity to the alkylating agent methyl methanesulfonate of a *rad52* mutant lacking the C-terminal domain [17]. In addition to a Rad51 binding domain, the C-terminus of human Rad52 has been shown to contain an RPA binding domain [22,23]. In this context, it is important to note that Rad52 is recruited to sites of DNA damage by RPA, whereas the recruitment of Rad51 and Rad59 is strictly dependent on Rad52 [24]. Both Rad52 and Rad59 accumulate into focal assemblies at DSBs. Co-immunoprecipitation experiments have identified both Rad51–Rad52–Rad59 and RPA–Rad52–Rad59 complexes, but no association of Rad59 with Rad51 or RPA is observed in the absence of Rad52 [19].

Genetic studies suggest that Rad52 and Rad59 have overlapping functions. Specifically, *rad52-R70K* and *rad59Δ* strains display synergistic sensitivity to γ-irradiation and a synergistic defect in meiosis [25]. Moreover, overexpression of Rad52 partially suppresses the γ-ray sensitivity of *rad59Δ* cells [8]. This view is supported by biochemical analyses, which show that both proteins bind DNA and stimulate DNA annealing [21,26–28]. Considering the absence of Rad51 and RPA binding domains in Rad59, it is not surprising that *rad52Δ* strains display a much more severe phenotype than *rad59Δ* strains and that overexpression of Rad59 cannot suppress a *rad52Δ* phenotype [8]. Consistent with these observations, Rad52 but not Rad59 catalyzes the annealing of RPA-bound ssDNA *in vitro* [28]. However, other functional differences between Rad59 and Rad52 may exist. In this study, we have analyzed the functional overlap and differences between these two proteins in HR and DNA DSB repair. Hence, we find that the N-terminus of Rad52 contains functions that are unique to Rad52 and we identify a number of amino acid residues in the N-terminus of Rad52 that are involved in functions that overlap with those of Rad59. The latter amino acid residues are likely involved in a novel common function of Rad52 and Rad59 since none of the amino acid residues are predicted to be located in the putative DNA binding groove of Rad52 or at the interface between individual Rad52 subunits.

2. Materials and methods

2.1. Media, strains and genetic methods

Yeast extract–peptone–dextrose (YPD) medium, synthetic complete (SC) medium and SC lacking specific amino acids were prepared as described previously [29]. Standard yeast manipulations were used for mating, sporulation, dissection and replica plating [30]. Lithium acetate transformation was employed [31]. All strains are *RAD5* derivatives of W303 (Supplementary Table).

The procedure of alanine substitution of residues in the Rad52 N-terminus was described previously [32]. Mutants of *RAD52* that display γ-ray sensitivity only in the *rad59Δ* background are analyzed in this study.

Selected mutants of Rad52 were fused to yellow fluorescent protein (YFP) or cyan fluorescent protein (CFP) and analyzed by fluorescence microscopy as described previously [33].

2.2. γ-Ray sensitivity

Plasmid-borne *rad52* mutants were transformed into a *rad52Δ rad59Δ* strain (W2081-1D). The transformants were tested for γ-ray sensitivity as described previously [32]. Mutations that lowered the survival by approximately 100-fold or more after exposure to 200 Gy compared to a transformant harboring a wild-type *RAD52* plasmid (pWJ1561) were designated class E mutants (for a description of class A through D mutants, see [32]) and selected for further analyses. Genomically integrated mutants were analyzed similarly except that cells were grown in YPD medium instead of SC–Trp. The LD_{37} was calculated as $-\ln(2.7)/\text{slope}$, where the slope is determined from the linear fit to the ln(% survival) versus γ-ray dose plot.

2.3. Mitotic recombination rates and direct-repeat recombination rates

Mitotic recombination between *leu2-ΔBstEII* and *leu2-ΔEcoRI* heteroalleles was measured in diploids as described previously [32] except that different media were used as indicated. The diploid strains, listed in Supplementary Table, were grown in SC medium before plating on SC-Leu plates.

The rate of *leu2* direct-repeat recombination was determined in haploid strains as described in [32] except that cells were grown in SC medium before plated on SC-Leu plates.

2.4. Construction of Rad59–Rad52 chimera plasmids

Chimera A consists of Rad59 residues 1–175 fused to Rad52 residues 169–504. Chimera B consists of full-length Rad59 fused to Rad52 residues 232–504. In brief, the chimera constructs were made as follows. First, sequences were amplified by PCR from pRS416-Rad59 [37] as a template and primers A: 5′-GGCGAATGGATGTTATAGAT-3′ and B: 5′-CTTCTTTAACGCATCGCCTA-3′ (fragment AB) or A: 5′-GGCG-AATGGATGTTATAGAT-3′ and C: 5′-GGCGAATGGATGTTA-TAGAT-3′ (fragment AC). Second, Rad52 fragments were amplified by PCR using pWJ1561 as a template with primer E: 5′-TAGGCGATGCGTTAAAGAAGTCTTTGAGAGGGTTTGGTAA-3′ and D: 5′-CGCGAATTCCGGGCGCTAACCTGGACCTTCTAGA-AGGCGGCCAGGAAGCGTTTCAAGTAGGC-3′ (fragment ED) or F: 5′-CTAAAGGCACGCATATCAAAAATAAAAGAAGGCAATTGAC-3′ and D: 5′-CGCGAATTCCGGGCGCTAACCTGGACCTTCTAGA-AGGCGGCCAGGAAGCGTTTCAAGTAGGC-3′ (fragment FD). Subsequently, the partially overlapping fragments AB and ED or AC and FD were fused in a second round of PCR using primers A and D. The resulting fragments ABED and ACFD were then digested by *XmaI* and *XbaI* and ligated into *XmaI* and *XbaI* digested pRS416-Rad59 [37] vector separately. The newly formed plasmids were digested with *MscI* and

*Bam*HI and each chimera Rad52–Rad59 containing fragment was isolated and ligated into the *SpeI* (end filled out by T4 polymerase)-*Bam*HI fragments of pWJ1561 and pWJ1562, respectively, to create pRS413-chimera A (pWJ1191), pRS413-chimera B (pWJ1193), pRS423-chimera A (pWJ1192), and pRS423-chimera B (pWJ1194). The expression plasmids were verified by sequencing.

To tag the chimeras with YFP, first a *CEN*-based plasmid pWJ1213 for expression of Rad52-YFP from its endogenous promoter was constructed by PCR-amplifying a *RAD52-YFP* fragment from strain W3749-14C [34] using primers Rad52-fwd2010 (5′-CCTTTGTTACAGCTAAGGC) and Rad52-down (5′-AATGAACCTAAGGATTCCGC). This fragment was cotransformed into yeast strain W1588-4C [35] for gap-repair with an *SphI* cut pRS413-Rad52 plasmid [32]. The gap-repaired plasmid (pWJ1213) was rescued from yeast and sequenced to confirm the correct reconstitution of the *RAD52-YFP* expression cassette. Next, plasmids pWJ1191 to pWJ1194 were digested with *PstI* and the chimera-containing fragments were gel-purified. Likewise, the pWJ1213 plasmid was digested with *NheI* and a fragment containing the 3′-end of *RAD52*, YFP and the *RAD52* teminator sequence was gel-purified. The two gel-purified restriction fragments were co-transformed into W1588-4C for gap-repair using the 320 bp and 1737 bp of flanking sequence homology on either side of *PstI* site. The resulting plasmids (pWJ1241 to pWJ1244) containing chimera A and B fused to YFP were rescued by preparation of genomic DNA [36] and transformation into DH10B competent *E. coli* cells. The constructs were verified by restriction analysis and transformed into appropriate yeast strains for analysis by fluorescence microscopy (see text).

To test the functionality of the YFP fusion proteins, pWJ1191–pWJ1194, pWJ1241–pWJ1244, pRS413, pWJ1564 and pWJ1565 were transformed into a *rad59Δ* strain (W3251-27D). Individual transformants were grown in SC-His medium and then spotted in 10-fold serial dilutions onto SC-His plates before exposure to γ-irradiation. All plasmids are listed in Supplementary Table.

2.5. Complementation tests, fluorescence microscopy and protein blotting

The chimera plasmids were transformed into W1588-4C (wild-type), W3251-27D (*rad59::LEU2*), W3537-34A (*rad52-207Δ*), W3744-10D (*rad52-327Δ*) or W2014-5C (*rad52::HIS5*) and γ-ray sensitivity was tested as described previously [32]. Likewise, the plasmids containing the YFP-tagged chimeras were transformed into W2312-11D (*RAD52-CFP*), W3744-10D (*rad52-327Δ*), W3537-34A (*rad52-207Δ*), W3777-17A (*rad52::HIS5*), W4970-10B (*RAD52-RFP rad59::HIS3*), W5867-2B (*CFP-RAD51 rad52::HIS5*) and W5843-2C (*CFP-RAD51*). W6640-3B (*RAD52-YFP CFP-RAD51*) acts as a control. Plasmids expressing chimeric proteins (pWJ1191–pWJ1194) were also transformed into UM56-1B (Rad52-207Δ-YFP) to examine localization. The transformants were then prepared for fluorescence microscopy as described [33]. DNA was visualized by staining live cells with 10 μg/ml DAPI for 30 min.

The expression level of chimera proteins was determined by protein blot analysis using an anti-Rad52 antibody as described previously [21].

3. Results

3.1. Construction of Rad59–Rad52 chimeras

First, we addressed the question of whether Rad59 is functionally equivalent to the conserved N-terminus of Rad52 [19,27,37]. To test this possibility, we constructed two chimeras of Rad59 and Rad52 in which the conserved Rad59 N-terminus or full-length Rad59 is extended with the Rad51 and RPA interacting C-terminal domain of Rad52 (Fig. 1A). In both cases, the final protein fusion was approximately the size of the full-length Rad52 protein. More specifically, chimera A consists of the Rad59 residues that are most homologous to Rad52 (1–175) fused at the site of homology to Rad52 (residues 169–504). Chimera B contains the entire Rad59 open reading frame fused to residues 232–504 of Rad52. If the chimeras are expressed and sort to the nucleus, and if the N-termini of Rad52 and Rad59 have identical and interchangeable functions, then each chimera is expected to behave like genuine Rad52 protein. On the other hand, if the N-termini of Rad52 and Rad59 have distinct functions, then, at the least, the chimeras should complement a *rad59∆* strain.

3.2. Rad59–Rad52 chimeras are expressed and sort to the nucleus

To test expression of the two chimeras, total cell extracts were prepared from the transformed strains and analyzed by protein blotting using an anti-Rad52 antibody (Fig. 1B). Both of the chimeras appear slightly larger than Rad52 as judged by their electrophoretic mobility (compare the chimeric proteins to the endogenous Rad52 band in the *rad59∆* strain in Fig. 1B). In the *rad59∆* strain, chimera A is only detected when it is expressed from a multi-copy plasmid, however a significant degradation band is also seen. Higher levels of chimera B are also seen when it is expressed from a multi-copy plasmid. In a *rad52∆* strain, chimera A is barely detected from either single or multi-copy plasmids and significant levels of chimera B are detected only when it is expressed from a multi-copy plasmid. These observations suggest that wild-type Rad52 protein aids in stabilizing the chimeras *in vivo*.

We have recently shown that Rad59 requires Rad52 for efficient nuclear localization [24]. Moreover, we have also identified a nuclear localization signal (NLS) of the pat7 type spanning residues 231–237, which is essential for the sorting of Rad52 to the nucleus (I. Plate, U. Mortensen, in preparation) [38]. Chimera A contains this NLS, but in chimera B the NLS is right at the Rad59–Rad52 junction and was changed from being a pat7 type to a conventional NLS-type during the construction [39]. Therefore, we tested whether both chimeras are correctly sorted to the nucleus by tagging them with YFP to determine their localization. The YFP-tagged chimeras behave similarly to the untagged chimeras in their complemention of the γ-ray sensitivity of a *rad59∆* strain (data not shown). In wild-type or *rad59∆* cells, ectopic expression of either chimera allows proper localization to the nucleus (Fig. 1C and data not shown). Consistent with the protein blot analysis, chimera A is barely detectable in *rad52∆* cells (Fig. 1D), while chimera B is readily detected in the nucleus (Fig. 1D).

3.3. Rad59–Rad52 chimeras complement the γ-ray sensitivity of rad59∆, but not of rad52∆ strains

To study the activity of the chimeras, we first investigated whether they provide Rad59 function. Single- or multi-copy plasmids expressing either of the chimeras were transformed into a *rad59∆* strain and the transformants tested for γ-ray sensitivity. Even the reduced chimera A protein levels expressed from a single-copy plasmid can partially rescue the γ-ray sensitivity of a *rad59∆* strain (Fig. 2A). In contrast, chimera B expression from a single copy plasmid fully rescues the γ-ray sensitivity of a *rad59∆* strain (Fig. 2A). Furthermore, both chimeras fully complement *rad59∆* when expressed from multi-copy plasmids (Fig. 2B). Therefore, we conclude that the function of Rad59 in γ-ray repair is maintained fully in chimera B, but partially in chimera A.

Next, the ability of the chimeras to complement the γ-ray sensitivity of a *rad52∆* strain was determined. Whether expressed from a single- or multi-copy plasmid, the chimeras completely fail to rescue the γ-ray sensitivity of a *rad52∆* strain (Fig. 2C and D). In light of the fact that expression of chimera B from a multi-copy plasmid results in near wild-type protein levels (compared to endogenous Rad52), we conclude that Rad59 cannot substitute for the functions normally provided by the N terminus of Rad52.

3.4. Rad59–Rad52 chimeras interact with Rad51 but are recruited inefficiently to sites of DNA damage

Next, we investigated whether the Rad52 portion of the chimera can engage Rad51 in DNA repair. Since the Rad52 segment of the chimera contains the Rad51 interaction domain, we tested whether Rad51 binding was functional in the two chimeras. Two-hybrid analysis indicates that chimera B, unlike Rad59 on its own, is capable of interacting with Rad51 although not as strongly as Rad52 (data not shown) [19]. However, this experiment does not reveal whether the interaction of chimera B with Rad51 is productive in DNA repair. To investigate this possibility, we took advantage of the fact that the DNA damage sensitivity of *rad52-207∆* and *rad52-327∆* truncation mutants lacking the Rad51 interaction domain can be rescued by intragenic complementation with *rad52-2*, which has a missense mutation in the Rad52 N-terminus [17,18]. This result shows that functions of Rad52 present in the N- and C-terminus can collaborate even when present in two different molecules, likely because the two mutant species form heteromeric rings.

Inspired by this observation, we tested whether the defects of strains expressing the *rad52* truncation mutants can be suppressed by co-expression of the Rad59–Rad52 chimeras. Hence, single- or multi-copy plasmids expressing the chimeras were transformed into *rad52-207∆* and *rad52-327∆* strains. The resulting transformants were tested for γ-ray sensitivity. As seen in Fig. 3A, the chimeras partially complement *rad52-327∆*, demonstrating that both can form a complex with *rad52-327∆* and bind Rad51 to reconstitute a proficient DSB repair machinery. In contrast, neither chimera complements *rad52-207∆* (Fig. 3B). The difference between the two *rad52* truncation mutants may be explained by the Rad52-207∆ protein lacking nuclear localization, while Rad52-327∆
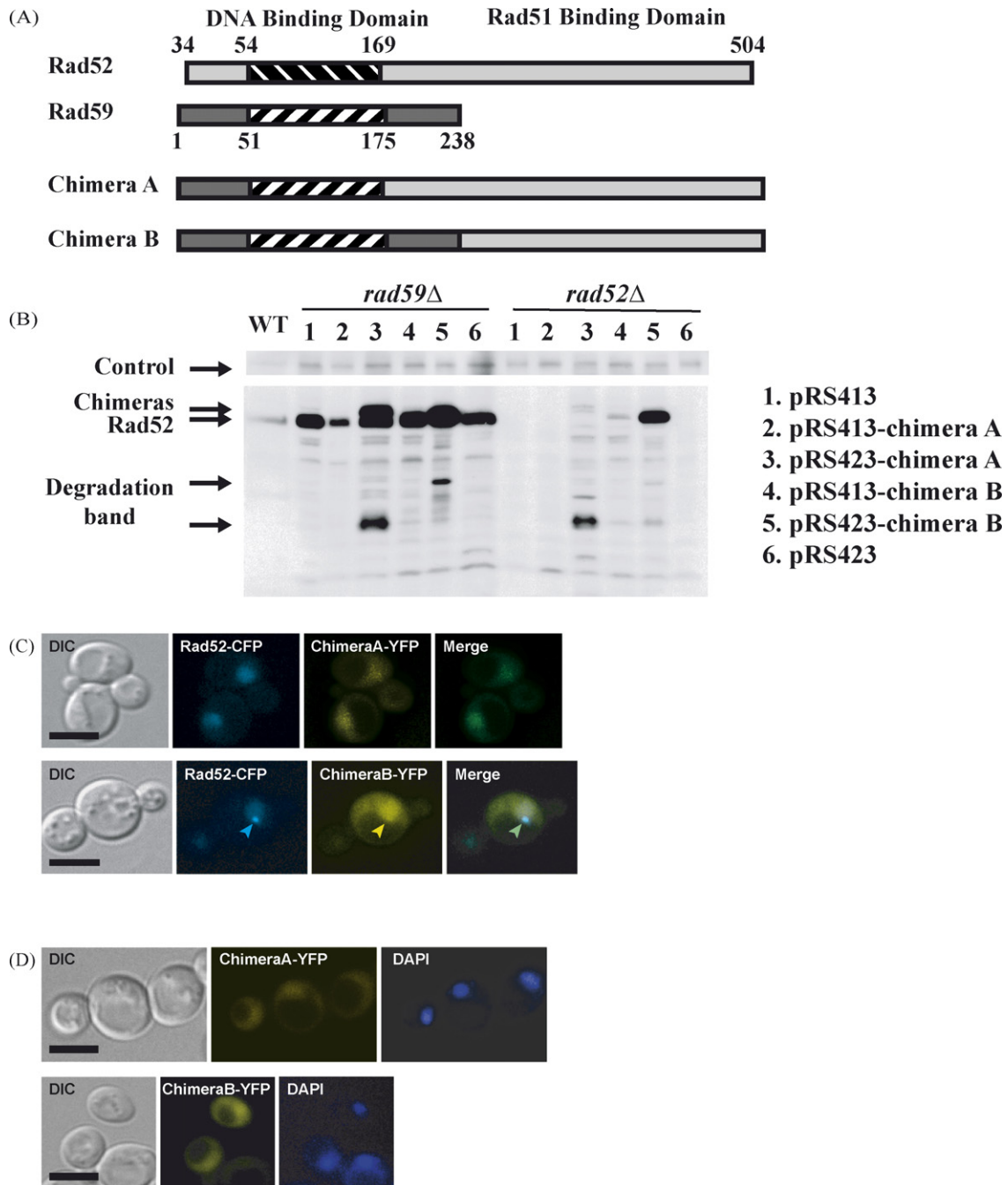
Fig. 1 – **Characterization of Rad59–Rad52 chimeric proteins and cellular localization of chimeras. (A) Chimera constructs. Rad59 shares 32% sequence identity and 53% similarity with the N-terminus of Rad52. Hatching indicates the highly conserved DNA binding domain and shading the less conserved amino acids. Chimera A consists of Rad59 residues 1–175 fused to Rad52 residues 169–504. Chimera B contains all of Rad59 fused to Rad52 residues 232–504. (B) Protein blot analysis of chimera proteins. Rad59–Rad52 chimeras expressed from single- or multi-copy vectors (pRS413 and pRS423, respectively) in *rad59Δ* or *rad52Δ* strains as indicated. A control cross-reacting protein is shown from an over-exposed film of the same gel. The endogenous wild-type Rad52 protein is visible both in WT and the *rad59Δ* strains. (C) Localization of chimera A and B expressed from a multi-copy plasmid in *RAD52* wild-type cells (W2312-11D). (D) Nuclear localization of chimeras in *rad52Δ* (W3777-17A). Scale bar, 3 μm.**

is proficient in nuclear recruitment (I. Plate, U. Mortensen, in preparation). Therefore, we tested the ability of the chimeras to support transport of Rad52-207Δ into the nucleus. For microscopy analysis, the chimera plasmids were individually transformed into a strain expressing Rad52-207Δ-YFP (UM56-1B). Inspection of the transformants shows that Rad52-207Δ, which on its own resides in the cytoplasm, is transported into the nucleus by the chimeras (data not shown). These results
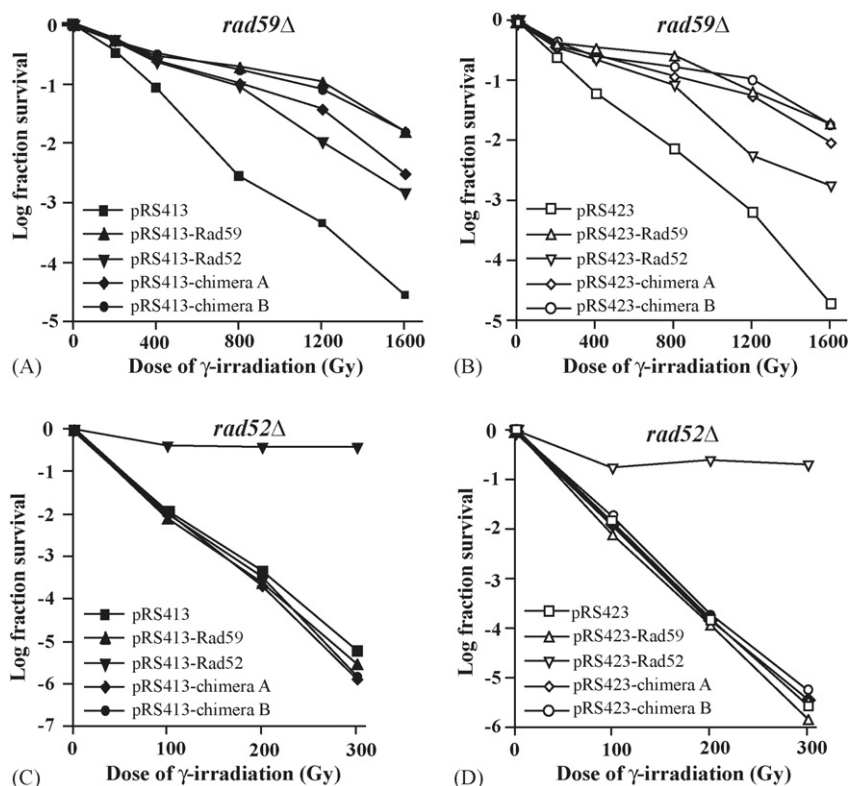
Fig. 2 – γ-Ray survival curves for Rad59–Rad52 chimeras expressed from single- or multi-copy vectors in *rad59Δ* or *rad52Δ* strains (W3251-27D and W2014-5C, respectively) as indicated. (A–D) ■, pRS413; ▲, pRS413-Rad59; ▼, pRS413-Rad52; ♦, pRS413-chimera-A; ●, pRS413-chimera-B; □, pRS423; △, pRS423-Rad59; ▽, pRS423-Rad52; ◇, pRS423-chimera-A; ○, pRS423-chimera-B.

indicate that the chimeras form a complex with the Rad52 truncations and are able to engage Rad51 in DNA repair. However, the chimeras lack functions other than those normally supplied by the Rad52 N-terminus.

Further, we tested whether the chimeras are recruited to sites of DNA repair by monitoring their localization relative to wild-type Rad52 tagged with cyan fluorescent protein (CFP) after exposing cells to 40 Gy of γ-irradiation. After this treatment, chimera B forms foci that co-localize with Rad52-CFP and CFP-Rad51 foci (data not shown). In *rad52Δ* cells, chimera B also forms foci after exposure to γ-irradiation, albeit less efficient (5% of budding cells) compared to wild-type (90%) (Fig. 3C and data not shown). All chimera B foci colocalized with CFP-Rad51 foci (Fig. 3C), further arguing that the repair defects of chimera B in *rad52Δ* cells are not due to a failure in binding Rad51. Taken together, we conclude that the chimera B does not form a fully functional "Rad52" protein due to the lack of functions normally supplied by the N-terminus of Rad52 and not provided by Rad59. The reduced efficiency of focus formation in response to γ-irradiation suggests that this function involves recruitment to the DNA lesion.

3.5. Identification of novel rad52 mutants with a synthetic genetic interaction with rad59Δ

To map the regions of Rad52 that have overlapping functions with Rad59, we screened a previously generated collection

of plasmid-borne site-specific point mutations in the Rad52 N-terminus for synthetic genetic interactions with *rad59Δ* in an assay for γ-ray sensitivity (see Section 2) [32]. This strategy identified nine mutants, *K61A, S68A, Y80F, R114A, Y182A, Y184A, K189A, Y192A,* and *K194A,* which display synergistic sensitivity to γ-irradiation in a *rad59Δ* background (Fig. 4). These mutants define a new class of *rad52* mutants referred to as class E (for a definition of class A, B, C and D mutations see [32]). The class E mutants were integrated into the genome for further characterization. First, survival curves were generated by exposing cells to various doses of γ-irradiation and scoring the percentage of surviving cells (Fig. 5 and data not shown). For the γ-ray survival curves, the corresponding LD_{37} was calculated as described in Section 2 (Table 1). Several of the identified mutants display stronger synthetic effects with *rad59Δ* compared to those described for *rad52-R70K,* the original mutant defining this class of *rad52* mutants [25]. The *rad52-R114A* single mutant is the most γ-ray resistant of the class E mutants with an LD_{37} indistinguishable from the wild-type. In contrast, the *rad52-R114A rad59Δ* double mutant is highly sensitive to γ-irradiation although not as sensitive as the *rad52Δ rad59Δ* double mutant (Table 1). At the other end of the spectrum, *rad52-Y182A* is the most γ-ray sensitive single mutant ($LD_{37} = 82 \pm 0.5$) and the *rad52-Y182A rad59* double mutant displays γ-ray sensitivity similar to the *rad52Δ rad59Δ* double null. The LD_{37} of the remaining class E *rad52* mutants fall in between these two
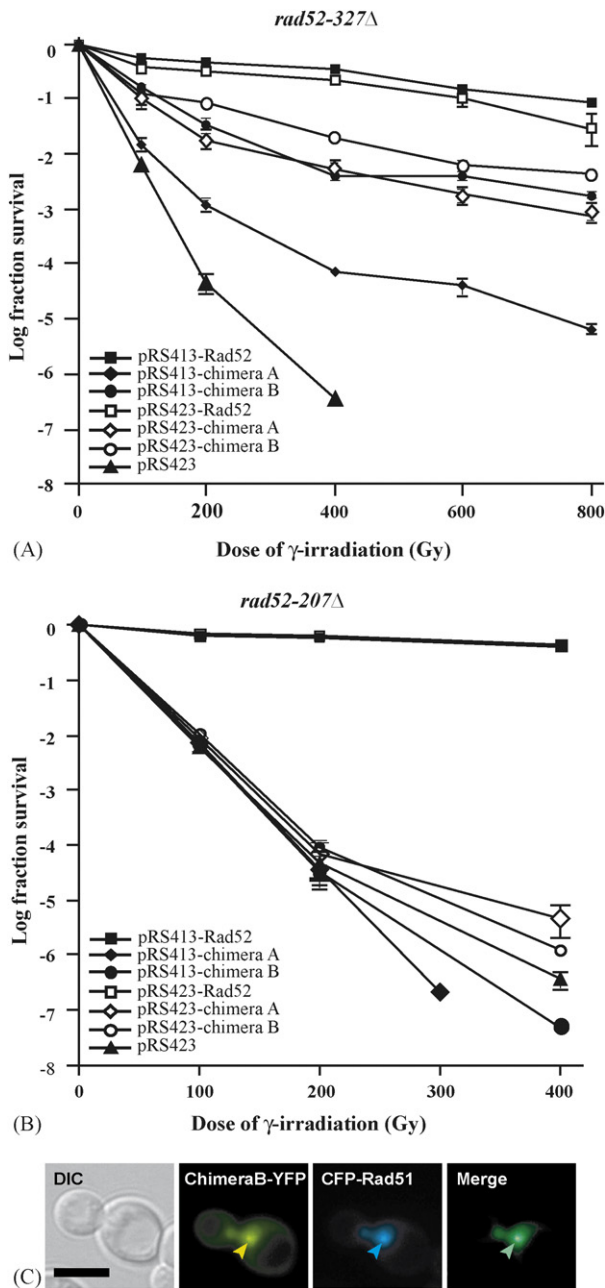
**Fig. 3 – Complementation of the γ-ray sensitivity of
rad52-207Δ (W3537-34A) and *rad52-327Δ* (W3744-10D) by
the chimeras. (A and B)** ■, pRS413-Rad52; ♦,
pRS413-chimera-A; ●, pRS413-chimera-B; □,
pRS423-Rad52; ◊, pRS423-chimera-A; ○,
pRS423-chimera-B; ▲, pRS423. **(C)** Localization of
2 μm-expressed chimera B in *CFP-RAD51 rad52Δ*
(W5867-2B) 30 min after exposure to 40 Gy of γ-irradiation.
Arrowheads mark co-localizing chimera B and Rad51 foci.
Scale bar, 3 μm.

mutants. Of the class E mutants, *rad52-K194A* displays the
largest difference in LD$_{37}$ between the wild-type and *rad59Δ*
background (nine-fold). Thus, the ensemble of class E amino
acid residues are required for a function, which is shared by
Rad59.

Next, the effect of the *rad52* class E mutations on spon-
taneous heteroallelic and direct-repeat recombination was
tested in both wild-type and *rad59Δ* genetic backgrounds
(Table 1). Surprisingly, no synthetic defect in recombination
was observed when class E mutations were combined with
rad59Δ. On the contrary, most of these double mutants dis-
played slightly elevated spontaneous recombination rates. In
summary, in *rad59Δ* strains, the *rad52* class E mutants fail
to repair γ-ray induced damage even though they readily
support mitotic homologous recombination. A similar sep-
aration of homologous recombination and repair of γ-ray-
induced DNA damage was previously described for another
class of *rad52* mutants (class C) [32]. However, in contrast to
rad52 class E mutants, the separation of function phenotype
of class C mutants can be observed even in the presence of
Rad59.

Both wild-type and *rad52* class C mutant cells form sponta-
neous Rad52 foci in S phase in agreement with their ability to
perform homologous recombination (Mortensen et al., PLoS
Genetics, submitted for publication). To test whether Rad52
class E mutant protein behaves similarly, four class E mutants,
rad52-S68A, *K182A*, *K189A*, and *K194A*, were tagged with YFP
and their distribution in the cell visualized by fluorescence
microscopy (Table 1). Similar to wild-type and Rad52 class C
mutants, the class E mutants form foci, indicating that the
mutant protein is recruited to sites of DNA damage to engage
in homologous recombination.

Overall, the *rad52* class E mutants uncover regions in the
Rad52 N-terminus that carry out essential functions in DNA
double-strand break repair that can also be performed by
Rad59. These functions are not essential for homologous inter-
chromosomal heteroallelic recombination although this pro-
cess may proceed slower in the absence of Rad59 as indicated
by the large number of cells containing recombination foci in
rad59Δ strains.

4. Discussion

4.1. Functional differences between the Rad52 and Rad59 N-termini

In this study, we use Rad59–Rad52 chimeric proteins to
demonstrate that the N-terminus of Rad52 provides unique
function(s) to DSB repair that cannot be replaced by Rad59. In
summary, the chimeras can complement the γ-ray sensitivity
of a *rad59Δ* strain but show no complementation of a *rad52Δ*
strain despite the fact that chimera B is expressed, recruited
to sites of DNA damage, and interacts with RPA, Rad52 and
Rad51. Interestingly, both chimeras can complement the γ-ray
sensitivity of *rad52-327Δ*, but not that of *rad52-207Δ*. Although
Rad52-207Δ does not contain a functional NLS, and does not
sort to the nucleus on its own (I. Plate, U. Mortensen, in prepa-
ration), Rad52-207Δ-YFP is localized to the nucleus in the
presence of both chimeras. Thus the lack of complementation
between *rad52-207Δ* and the chimeras cannot be explained
by a failure of Rad52-207Δ to localize to the nucleus indicat-
ing that the chimeras form complexes with the truncated
Rad52 species. Furthermore, the γ-ray sensitivity of strains
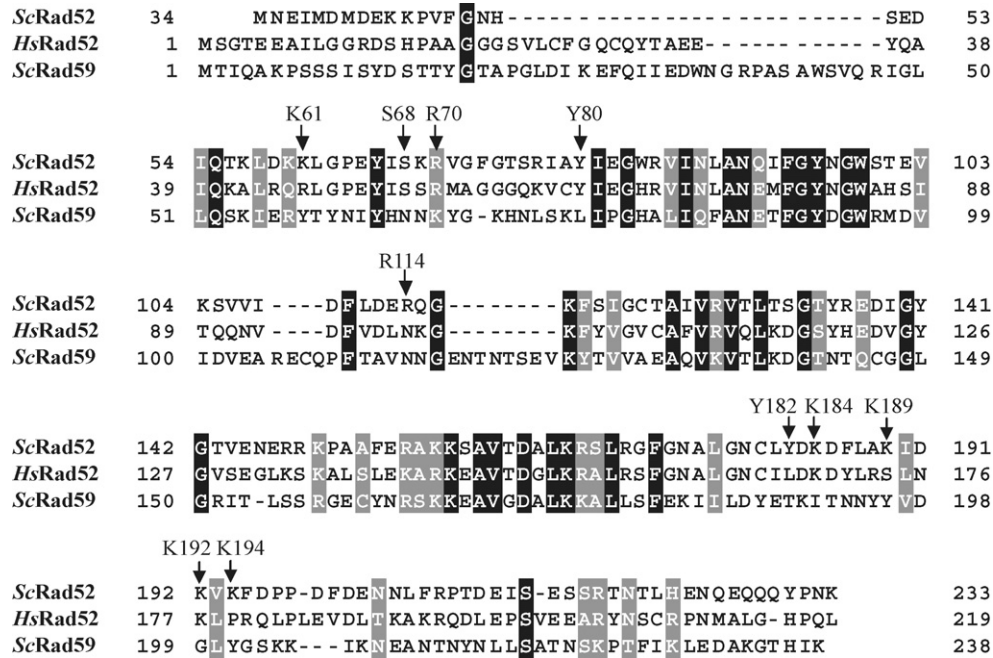expressing the chimera-Rad52-207Δ complexes, suggests

Fig. 4 – Alignment of Rad52 and Rad59 amino acid sequences. Identity indicated by black shading and similarity by grey shading. Alanine substituted residues with a synthetic genetic interaction with *rad59Δ* are marked by arrowheads.

that the truncated Rad52-207Δ protein does not benefit from the functional domains present in Rad52 amino acid residues 232–504 when they are recruited via the Rad59 portion of the chimera. We also observe that chimera B is inefficient at forming repair foci after exposure to γ-irradiation. This is consistent with the DNA repair defect of the chimeras and further indicates that functions normally supplied by the N-terminus of Rad52 are not provided by Rad59 to ensure efficient recruitment of the chimeras to γ-ray-induced DNA damage.

4.2. Novel rad52 mutants

In addition to differences between Rad52 and Rad59, we identify nine mutations in *RAD52*, collectively referred to as class E, which confer synergistic γ-ray sensitivity with a *rad59Δ* deletion, indicating that these residues encode functions common to the two proteins. The mutated residues lie within the highly conserved N-terminus of Rad52, but are not particularly conserved themselves. The low degree of evolutionary conservation among the mutated residues is consistent with

Table 1 – Effect of *rad52* and *rad52 rad59Δ* mutants on γ-ray sensitivity and mitotic heteroallelic and direct-repeat recombination

Allele	γ-Ray sensitivity (LD$_{37}$)[a]		Heteroallelic recombination rate ($\times 10^{-8}$)[b]		Direct-repeat recombination ($\times 10^{-6}$)[b]		Spontaneous Rad52 focus[d] (% cells) (G1)/(S/G2/M)	
	RAD59	rad59Δ	RAD59	rad59Δ	RAD59	Rad59Δ	RAD59	rad59Δ
RAD52	392 ± 74	173 ± 7	102 ± 15	214 ± 27	45.3 ± 11.6	25.2 ± 6.9	0/14	4.7/39.3
rad52Δ	19 ± 0.1	21 ± 1	0.6 ± 0.3	1.8 ± 0.5	1.5 ± 0.4	2.5 ± 0.7	0	0
K61A	105 ± 4	30 ± 1	ND[c]	ND	33.7 ± 9.6	42.2 ± 10.4	ND	ND
S68A	116 ± 14	24 ± 1	127 ± 22	180 ± 26	46.6 ± 11.4	24.4 ± 8.9	0.7/24.1	1.2/39.8
Y80F	156 ± 17	26 ± 1	ND	ND	26.4 ± 9.0	18.3 ± 6.1	ND	ND
R114A	528 ± 73	67 ± 4	140 ± 23	400 ± 47	78.8 ± 25.3	38.5 ± 13.2	ND	ND
Y182A	82 ± 5	33 ± 3	ND	ND	96.6 ± 30.7	49.8 ± 17.0	0.2/34.2	0.7/39.2
Y184A	137 ± 8	28 ± 2	212 ± 35	400 ± 52	53.3 ± 16.6	40.5 ± 16.6	ND	ND
K189A	260 ± 53	42 ± 3	ND	ND	54.3 ± 17.5	36.9 ± 12.9	1.6/9.8	0.4/33.3
Y192A	198 ± 15	28 ± 3	ND	ND	65.8 ± 16.0	21.9 ± 7.2	ND	ND
K194A	325 ± 50	37 ± 3	206 ± 32	440 ± 59	51.0 ± 12.5	46.1 ± 14.1	0.6/14.6	0.7/58.7

[a] LD$_{37}$ in Gy calculated as described in Section 2.
[b] Recombination rate is presented as events per cell per generation as described previously [32].
[c] Not determined.
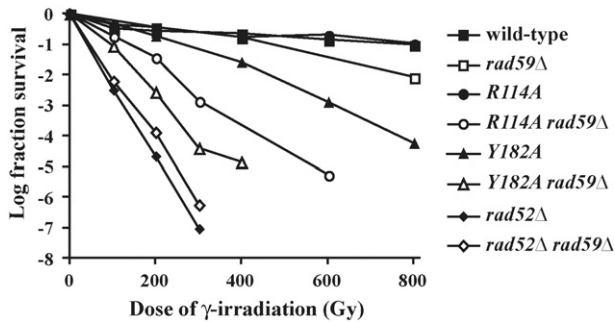[d] The percentage of cells of the indicated cell cycle stage that have a Rad52 focus(i).

Fig. 5 – Synergistic γ-ray sensitivity between *rad59Δ* and *rad52* class E mutants. ■, wild-type (W1588-4C); □, *rad59Δ* (W3251-27D); ●, *rad52*-R114A (J767); ○, *rad52*-R114A *rad59Δ* (W5394-7D); ▲, *rad52*-Y182A (J775); △, *rad52*-Y182A *rad59Δ* (W5377-1A); ♦, *rad52Δ* (W2014-5C); ◇, *rad52Δ rad59Δ* (W2081-1D).

their mild phenotype in an otherwise wild-type genetic background. The severity of the mutations in a *rad59Δ* background suggests that the defects conferred by the mutations can be complemented by Rad59 function.

In human Rad52, the amino acid residue that corresponds to R70 in *S. cerevisiae*, is involved in binding of single-stranded DNA and when mutated to alanine, DNA binding is severely reduced [14,40]. In *S. cerevisiae*, a *rad52*-R70A strain qualifies as a class C mutant and is therefore very γ-ray sensitive even in the presence of Rad59. Hence, strongly compromised DNA binding in Rad52 is unlikely to be rescued by Rad59. In a *rad52*-R70K mutant, which is the founder of the class E mutants [25],

an arginine residue is mutated to the chemically similar lysine residue. Likely, DNA binding is less affected in Rad52-R70K compared to Rad52-R70A where the positively charged arginine is changed to a small and neutral alanine residue. This difference may explain why DNA repair is compromised in the R70K protein only in the absence of Rad59. We therefore speculate that Rad59 rescues the defect of Rad52-R70K by stabilizing a weakened interaction with the DNA lesion. In this context it is interesting to note that by studying the dependency of direct repeat recombination on Rad59, Sugawara and colleagues also suggested that Rad59 acts by stabilizing recombination intermediates [41]. Possibly, this type of stabilization could be mediated via strand-annealing, which is a common activity of Rad52 and Rad59. Moreover, stabilization of Rad52 binding to a recombination substrate by Rad59 may be mediated via the ability of Rad59 to interact directly with Rad52, perhaps even by being fully integrated in a ring structure otherwise composed of Rad52 subunits [37,42].

The human amino acid residues corresponding to the class E mutations discovered in this study map to the surface of the undecameric ring or at the base of the DNA binding groove in the structure of Rad52 [14] (Fig. 6). The class E mutations are therefore more likely to affect interaction with other proteins or with DNA rather than monomer-monomer interaction. Interestingly, two of the class E mutations (Y80F and K184A) severely reduce single-stranded DNA binding of human Rad52 [14,40] although neither appears to be in direct contact with single-stranded DNA in the predicted structure [15]. This suggests that a wider range of residues in Rad52 contributes to efficient DNA binding. This interpretation is corroborated by the class C mutations, which all map to the putative DNA binding groove in the human structure of Rad52 and have a
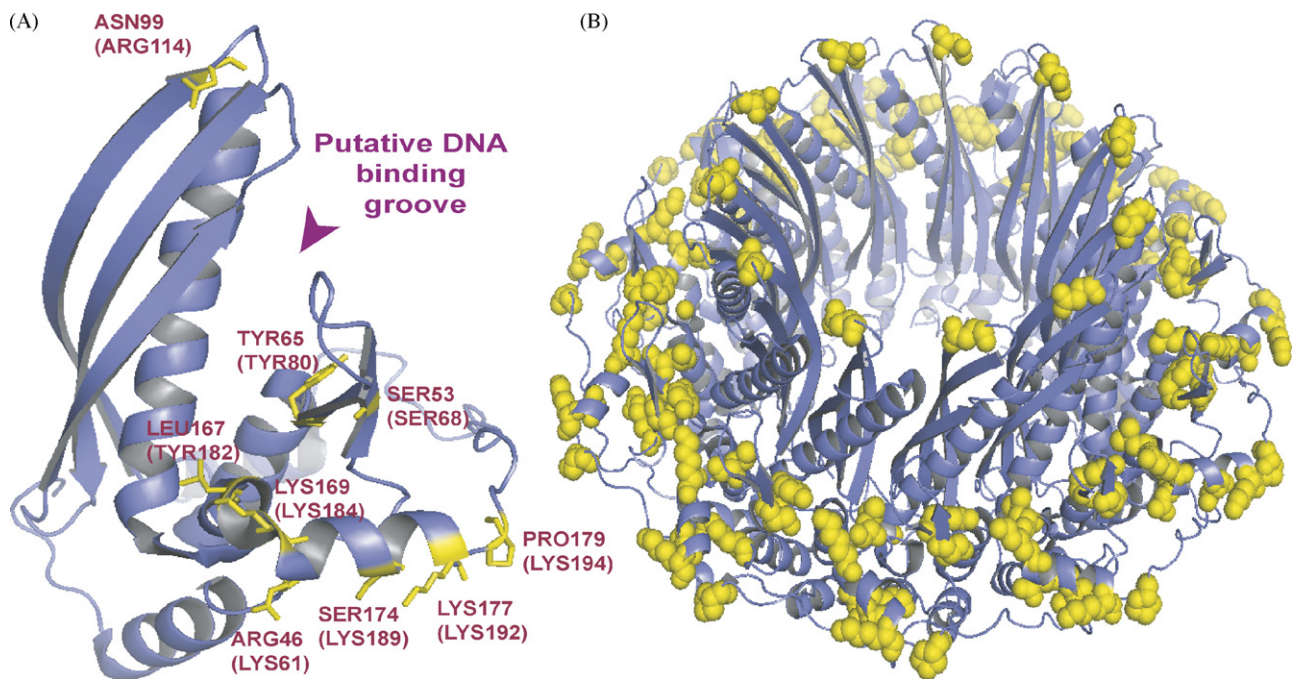

Fig. 6 – Modeling of *rad52* class E mutations into the structure of human Rad52 (protein data bank ID 1KN0). The figures were created using Pymol software. (A) *Hs*Rad52 monomer. Labels indicate human amino acid residues and the corresponding *S. cerevisiae* residues in parentheses. (B) *Hs*Rad52 heptameric ring. Mutant residues showing a synergistic defect with *rad59Δ* are shown in yellow.

separation of function phenotype similar to that of the class E mutants in a *rad59Δ* background [32].

4.3. Concluding remarks

Based on the sum of evidence, we propose that binding of Rad52 to a DNA lesion is a multi-step process, where Rad52 is first recruited to the DNA lesion by its RPA interaction even in the absence of a functional DNA binding domain in the N-terminus [24]. In agreement with this view, we have previously observed that Rad52-C180A, a class C mutant, can be recruited to a DNA double-strand break but fail to complete repair (Mortensen et al., PLoS Genetics, 2006 submitted for publication). All class E mutants spontaneously form repair foci during the cell cycle indicating that they are recruited to sites of DNA damage. After recruitment by RPA, efficient DNA binding/annealing by Rad52 requires both a functional DNA binding groove (defective in class C mutants), which cannot be substituted by Rad59, and a second function (defective in class E mutants), which can be complemented by Rad59. This latter function could be a conformational change or an initial interaction with DNA guiding it to the DNA binding groove or stabilizing the bound DNA.

Acknowledgments

Appendix A. Supplementary data

Supplementary data associated with this article can be found, in the online version, at doi:10.1016/j.dnarep.2006.08.007.

REFERENCES

[1] F. Paques, J.E. Haber, Multiple pathways of recombination induced by double-strand breaks in *Saccharomyces cerevisiae*, Microbiol. Mol. Biol. Rev. 63 (1999) 349–404.

[2] P. Sung, Function of yeast Rad52 protein as a mediator between replication protein A and the Rad51 recombinase, J. Biol. Chem. 272 (1997) 28194–28197.

[3] L. Krejci, B. Song, W. Bussen, R. Rothstein, U.H. Mortensen, P. Sung, Interaction with Rad51 is indispensable for recombination mediator function of Rad52, J. Biol. Chem. 277 (2002) 40132–40141.

[4] B. Song, P. Sung, Functional interactions among yeast Rad51 recombinase, Rad52 mediator, and replication protein A in DNA strand exchange, J. Biol. Chem. 275 (2000) 15895–15904.

[5] J.H. New, T. Sugiyama, E. Zaitseva, S.C. Kowalczykowski, Rad52 protein stimulates DNA strand exchange by Rad51 and replication protein A, Nature 391 (1998) 407–410.

[6] A. Shinohara, T. Ogawa, Stimulation by Rad52 of yeast Rad51-mediated recombination, Nature 391 (1998) 404–407.

[7] F.E. Benson, P. Baumann, S.C. West, Synergistic actions of Rad51 and Rad52 in recombination and DNA repair, Nature 391 (1998) 401–404.

[8] Y. Bai, L.S. Symington, A Rad52 homolog is required for *RAD51*-independent mitotic recombination in *Saccharomyces cerevisiae*, Genes Dev. 10 (1996) 2025–2037.

[9] Q. Chen, A. Ijpma, C.W. Greider, Two survivor pathways that allow growth in the absence of telomerase are generated by distinct telomere recombination events, Mol. Cell. Biol. 21 (2001) 1819–1827.

[10] M.B. Vaze, A. Pellicioli, S.E. Lee, G. Ira, G. Liberi, A. Arbel-Eden, et al., Recovery from checkpoint-mediated arrest after repair of a double-strand break requires Srs2 helicase, Mol. Cell. 10 (2002) 373–385.

[11] F.S. Dietrich, S. Voegeli, S. Brachat, A. Lerch, K. Gates, S. Steiner, et al., The *Ashbya gossypii* genome as a tool for mapping the ancient *Saccharomyces cerevisiae* genome, Science 304 (2004) 304–307.

[12] M. van den Bosch, J.B. Zonneveld, P.H. Lohman, A. Pastink, Isolation and characterization of the *RAD59* homologue of *Kluyveromyces lactis*, Curr. Genet. 39 (2001) 305–310.

[13] S. Hamimes, H. Arakawa, A.Z. Stasiak, A.M. Kierzek, S. Hirano, Y.G. Yang, et al., RDM1, a novel RNA recognition motif (RRM)-containing protein involved in the cell response to cisplatin in vertebrates, J. Biol. Chem. 280 (2005) 9225–9235.

[14] W. Kagawa, H. Kurumizaka, R. Ishitani, S. Fukai, O. Nureki, T. Shibata, et al., Crystal structure of the homologous-pairing domain from the human Rad52 recombinase in the undecameric form, Mol. Cell. 10 (2002) 359–371.

[15] M.R. Singleton, L.M. Wentzell, Y. Liu, S.C. West, D.B. Wigley, W. Kagawa, et al., Structure of the single-strand annealing domain of human RAD52 protein crystal structure of the homologous-pairing domain from the human Rad52 recombinase in the undecameric form, Proc. Natl. Acad. Sci. U.S.A. 99 (2002) 13492–13497.

[16] A.Z. Stasiak, E. Larquet, A. Stasiak, S. Muller, A. Engel, E. Van Dyck, et al., The human Rad52 protein exists as a heptameric ring, Curr. Biol. 10 (2000) 337–340.

[17] E.N. Asleson, R.J. Okagaki, D.M. Livingston, A core activity associated with the N terminus of the yeast *RAD52* protein is revealed by *RAD51* overexpression suppression of C-terminal *rad52* truncation alleles, Genetics 153 (1999) 681–692.

[18] K.L. Boundy-Mills, D.M. Livingston, A *Saccharomyces cerevisiae* *RAD52* allele expressing a C-terminal truncation protein: activities and intragenic complementation of missense mutations, Genetics 133 (1993) 33–49.

[19] A.P. Davis, L.S. Symington, The Rad52-Rad59 complex interacts with Rad51 and replication protein A, DNA Repair (Amst) 2 (2003) 1127–1134.

[20] G.T. Milne, D.T. Weaver, Dominant negative alleles of *RAD52* reveal a DNA repair/recombination complex including Rad51 and Rad52, Genes Dev. 7 (1993) 1755–1765.

[21] U.H. Mortensen, C. Bendixen, I. Sunjevaric, R. Rothstein, DNA strand annealing is promoted by the yeast Rad52 protein, Proc. Natl. Acad. Sci. U.S.A. 93 (1996) 10729–10734.

[22] L. Krejci, S. Van Komen, Y. Li, J. Villemain, M.S. Reddy, H. Klein, et al., DNA helicase Srs2 disrupts the Rad51 presynaptic filament, Nature 423 (2003) 305–309.

[23] M.S. Park, D.L. Ludwig, E. Stigger, S.H. Lee, Physical interaction between human *RAD52* and *RPA* is required for homologous recombination in mammalian cells, J. Biol. Chem. 271 (1996) 18996–19000.

[24] M. Lisby, J.H. Barlow, R.C. Burgess, R. Rothstein, Choreography of the DNA damage response; spatiotemporal relationships among checkpoint and repair proteins, Cell 118 (2004) 699–713.

[25] Y. Bai, A.P. Davis, L.S. Symington, A novel allele of *RAD52* that causes severe DNA repair and recombination deficiencies only in the absence of *RAD51* or *RAD59*, Genetics 153 (1999) 1117–1130.

[26] T. Sugiyama, J.H. New, S.C. Kowalczykowski, DNA annealing by *RAD52* protein is stimulated by specific interaction with the complex of replication protein A and single-stranded DNA, Proc. Natl. Acad. Sci. U.S.A. 95 (1998) 6049–6054.

[27] G. Petukhova, S.A. Stratton, P. Sung, Single strand DNA binding and annealing activities in the yeast recombination factor Rad59, J. Biol. Chem. 274 (1999) 33839–33842.

[28] Y. Wu, T. Sugiyama, S.C. Kowalczykowski, DNA annealing mediated by Rad52 and Rad59 proteins, J. Biol. Chem. 281 (2006) 15441–15449.

[29] F. Sherman, Getting Started with Yeast, vol. 194, Academic Press, Inc., San Diego, 1991.

[30] F. Sherman, G.R. Fink, J.B. Hicks, Methods in Yeast Genetics, Cold Spring Harbor Laboratory, Cold Spring Harbor, NY, 1986.

[31] H. Ito, K. Fukada, A. Murata, Kimura, Transformation of intact yeast cells treated with alkali cations, J. Bacteriol. 153 (1983) 163–168.

[32] U.H. Mortensen, N. Erdeniz, Q. Feng, R. Rothstein, A molecular genetic dissection of the evolutionarily conserved N terminus of yeast Rad52, Genetics 161 (2002) 549–562.

[33] M. Lisby, R. Rothstein, U.H. Mortensen, Rad52 forms DNA repair and recombination centers during S phase, Proc. Natl. Acad. Sci. U.S.A. 98 (2001) 8276–8282.

[34] M. Lisby, U.H. Mortensen, R. Rothstein, Colocalization of multiple DNA double-strand breaks at a single Rad52 repair centre, Nat. Cell. Biol. 5 (2003) 572–577.

[35] X. Zhao, E.G. Muller, R. Rothstein, A suppressor of two essential checkpoint genes identifies a novel protein that negatively affects dNTP pools, Mol. Cell 2 (1998) 329–340.

[36] C.S. Hoffman, F. Winston, A 10-min DNA preparation efficiently releases autonomous plasmids for transformation of *Escherichia coli*, Gene 57 (1987) 267–272.

[37] A.P. Davis, L.S. Symington, The yeast recombinational repair protein Rad59 interacts with Rad52 and stimulates single-strand annealing, Genetics 159 (2001) 515–525.

[38] G.R. Hicks, N.V. Raikhel, Protein import into the nucleus: an integrated view, Annu. Rev. Cell. Dev. Biol. 11 (1995) 155–188.

[39] D.A. Jans, C.K. Chan, S. Huebner, Signals mediating nuclear targeting and their regulation: application in drug delivery, Med. Res. Rev. 18 (1998) 189–223.

[40] J.A. Lloyd, D.A. McGrew, K.L. Knight, Identification of residues important for DNA binding in the full-length human Rad52 protein, J. Mol. Biol. 345 (2005) 239–249.

[41] N. Sugawara, G. Ira, J.E. Haber, DNA length dependence of the single-strand annealing pathway and the role of *Saccharomyces cerevisiae RAD59* in double-strand break repair, Mol. Cell. Biol. 20 (2000) 5300–5309.

[42] F. Cortes-Ledesma, F. Malagon, A. Aguilera, A novel yeast mutation, *rad52-L89F*, causes a specific defect in Rad51-independent recombination that correlates with a reduced ability of Rad52-L89F to interact with Rad59, Genetics 168 (2004) 553–557.